IOPscience iopscience.iop.org

Home Search Collections Journals About Contact us My IOPscience

Improvement in Crystalline Quality of InGaN-Based Epilayer on Sapphire via Nanoscaled Epitaxial Lateral Overgrowth

This content has been downloaded from IOPscience. Please scroll down to see the full text.

2010 Jpn. J. Appl. Phys. 49 105501

(http://iopscience.iop.org/1347-4065/49/10R/105501)

View the table of contents for this issue, or go to the journal homepage for more

Download details:

IP Address: 140.113.38.11
This content was downloaded on 25/04/2014 at 06:06

Please note that terms and conditions apply.

Improvement in Crystalline Quality of InGaN-Based Epilayer on Sapphire via Nanoscaled Epitaxial Lateral Overgrowth

Ching-Hsueh Chiu, Da-Wei Lin, Zhen-Yu Li, Chin-Hua Chiu, Chu-Li Chao, Chia-Cheng Tu[1], Hao-Chung Kuo*, Tien-Chang Lu, and Shing-Chung Wang

Department of Photonics and Institute of Electro-Optical Engineering, National Chiao Tung University, 1001 Ta Hsueh Road, Hsinchu 30010, Taiwan

[1]*Department of Electronic Engineering, Faculty of Engineering, Chung Yuan Christian University, Chungli 32023, Taiwan*

Received November 20, 2009; revised March 31, 2010; accepted May 21, 2010; published online October 20, 2010

In this study, a high-performance GaN-based light-emitting diode (LED) was achieved using a nanocolumn patterned sapphire substrate (NCPSS) with low-pressure metal-organic chemical vapor deposition (LP-MOCVD). The surface roughness was evaluated by atomic force microscopy (AFM). The mechanisms of carrier localization in the GaN-based LED fabricated on NCPSS were discussed referring to the results obtained from the power-dependent photoluminescence measurements. Moreover, from the transmission electron microscopy (TEM) image, the threading dislocation densities (TDDs) through the GaN-based LED fabricated on NCPSS were found to be about 10 times lower than those fabricated on planar substrates. Finally, the internal quantum efficiency (IQE) of the GaN-based LED fabricated on NCPSS was as high as 48% at 30 mW, corresponding to a current of 20 mA, which is higher than that of a GaN-based LED fabricated on a planar sapphire substrate by 8%. The use of NCPSS is suggested to be effective for elevating the emission efficiency of the GaN-based LED owing to an improvement in crystal quality.
© 2010 The Japan Society of Applied Physics

DOI: 10.1143/JJAP.49.105501

1. Introduction

High-brightness GaN-based light-emitting diodes (LEDs) with luminescence covering the range from infrared to ultraviolet (0.7 to 6.2 eV) have been extensively applied in, for example, large full-color displays, short-haul optical communication, traffic and signal lights, backlight for liquid-crystal displays, and common light fixtures.[1)] To satisfy next-generation applications in projectors, automobile head-lights, and high-end light fixtures, further improvements of the optical power and the external quantum efficiency are required. Typically, a GaN-based epilayer is grown on a planar sapphire substrate by heteroepitaxial techniques, such as metal-organic chemical vapor deposition (MOCVD).[2,3)] However, up to now, the GaN-based epilayer has had a high threading dislocation density (approximately 10^8–10^{10} cm^{-2}) owing to the large lattice mismatch and thermal expansion coefficient misfit.[4)] In the past, a number of investigations revealed that many properties of GaN-based LEDs and/or laser diodes (LDs) are affected by the threading dislocation density (TDD); for example, the efficiency and the lifetime of GaN-based LEDs and LDs decrease with increasing TDD of the GaN-based epilayer. In other words, the carriers in the GaN-based epilayer can leak through these threading dislocations and recombine nonradiatively. Therefore, it is very important to grow high-quality and low-TDD GaN-based epilayers. In the past decade, there have been many studies focused on improving the crystalline quality of the GaN-based epilayer, and attempts to grow an ultraflat-surface, low-TDD and high-crystalline-quality GaN-based epilayer on a sapphire substrate, for example, epitaxial lateral overgrowth (ELO)[5,6)] and cantilever epitaxy (CE)[7)] and using a microscale SiNx or SiOx patterned masks[8–10)] and a patterned sapphire substrate (PSS).[11–17)]

In this study, nanotechnology was used to form a nanocolumn patterned sapphire substrate (NCPSS) for the nanoscale epitaxial lateral overgrowth (NELO) of the GaN epilayer. Therefore, the suitable sapphire substrate with a nanoscale patterned surface for achieving a high-quality GaN-based epilayer is identified by comparing the structural and optical properties of specimens grown on planar sapphire substrates. In addition, the effects of NCPSS on the epitaxial structure of a GaN-based LED grown by low-pressure metal-organic chemical vapor deposition (LP-MOCVD) are systematically analyzed.

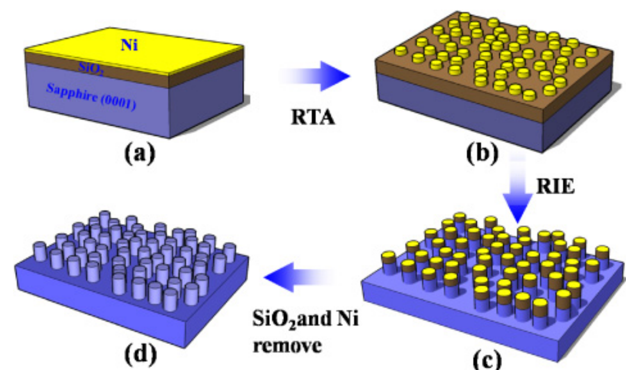

Fig. 1. (Color online) Fabrication flowchart of nanocolumn patterned sapphire substrate (NCPSS).

2. Experimental Procedure

The preparation of the GaN-based LED epilayer on NAPSS was as follows. First, a 200-nm-thick SiO_2 layer was deposited on the surface of the sapphire substrate by plasma-enhanced chemical vapor deposition (PECVD). Then, a 10-nm-thick Ni layer was deposited on the surface of the SiO_2 layer using an E-gun evaporator, as shown in Fig. 1(a). Next, the specimens were subjected to rapid thermal annealing (RTA) under flowing N_2 at temperatures of 850 °C for 1 min to form self-assembled Ni metal clusters, as shown in Fig. 1(b), which served as the mask for forming a SiO_2 nanocolumn by reactive ion etching (RIE) for 3 min. The pattern of the SiO_2 nanocolumn was then transferred to the sapphire substrate by RIE, as shown in Fig. 1(c). Finally, the residual Ni and SiO_2 on the specimen were removed using heated nitric acid solution (HNO_3) and buffered oxide

*E-mail address: hckuo@faculty.nctu.edu.tw

 © 2010 The Japan Society of Applied Physics

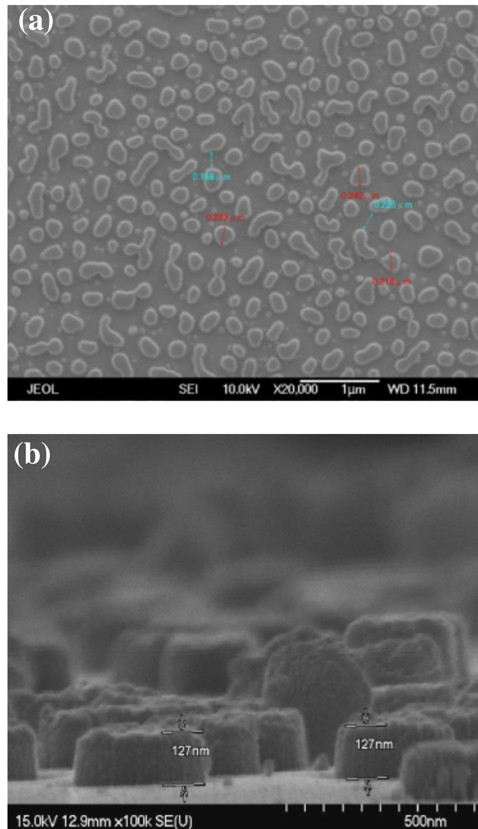

Fig. 2. (Color online) SEM images of NCPSS: (a) surface image; (b) cross-sectional image.

etch (BOE) solution, respectively, as shown in Fig. 1(d). The fabrication flowchart of NCPSS is shown in Figs. 1(a)–1(d). For our NCPSS, we also took SEM images from the top surface and the cross section of the specimens. In Fig. 2(a), we can clearly see that the nanocolumns (NCs) are vertically aligned and uniformly distributed over the entire surface, and the diameter of NCs is about 100–200 nm. Additionally, the cross-sectional SEM image of NCs is shown in Fig. 2(b), and the height of NCs is approximately 120–150 nm. Therefore, we can fabricate a NCPSS successfully. Secondly, following NCPSS fabrication, the epilayers of the GaN-based LED were fabricated on NCPSS by LP-MOCVD with a vertical reactor (Veeco D75) system. The metal-organic compounds of TMG, TMI, Cp_2Mg, gaseous NH_3, and SiH_4 were employed as the reactant source materials for Ga, In, Mg, N, and Si, respectively. The epitaxial structure of the GaN-based LED investigated is depicted in Fig. 3, and comprises a 30-nm-thick GaN nucleation layer, a 0.5-μm-thick undoped GaN epilayer, a 3-μm-thick n-GaN epilayer, a ten-period InGaN/GaN active layer, and a 0.2-μm-thick p-GaN contact layer. Moreover, we used the high-resolution XRD experimental and fitted scans of InGaN/GaN MQWs grown on the planar substrate and NCPSS. The calculated thicknesses of the well and barrier for the two samples are estimated to be the same: 3 nm for the well and 10 nm for the barrier.

The surface morphology of the specimen was observed by atomic force microscopy (AFM). The optical properties were investigated by power-dependent photoluminescence (PL) measurements. In this case, the PL measurement was excited with a frequency-tripled Ti:sapphire laser at a wavelength of 266 nm and a laser output power of 20 mW.

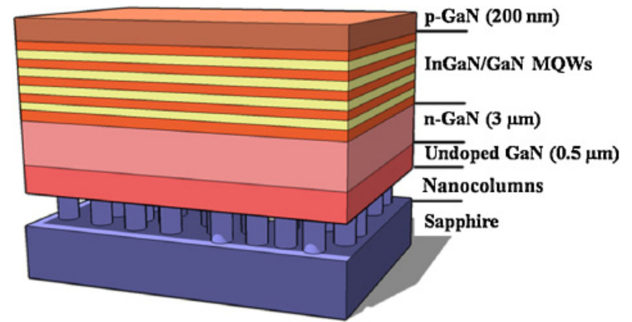

Fig. 3. (Color online) Schematics of epitaxial structures of GaN-based LED.

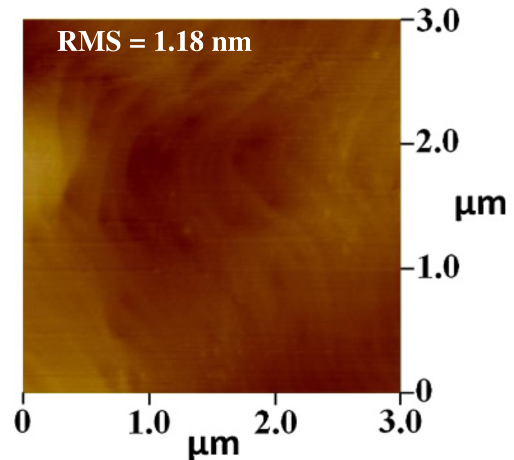

Fig. 4. (Color online) AFM images of GaN-based LED on NCPSS.

The laser pulse width was 200 fs and the repetition rate was 76 MHz. The luminescence spectrum was measured with a 0.5 m monochromator and detected with a photomultiplier tube. The distribution and threading behaviors of dislocations in the epilayer were then studied by transmission electron microscopy (TEM). Moreover, the interfacial microstructures of the epilayer were observed by high-resolution TEM. Finally, we used the power-dependent PL measurement to estimate the internal quantum efficiency (IQE) of specimens.

3. Results and Discussion

As shown in Fig. 4, the surface morphology of the top layer was observed by AFM, and no cracks were found. In addition, in our experiment, we believed that the GaN-based epilayer grown on NCPSS has a rougher surface compared with the GaN-based epilayer grown on the planar sapphire substrate. This is because the growth mechanism for the GaN-based epilayer on NCPSS is different from that on the planar sapphire substrate. In other words, we obtained a very small RMS value of the surface roughness of 1.18 nm, indicating that a high-quality GaN-based LED was successfully fabricated on NCPSS.

Figure 5 shows the PL spectra of the GaN-based LED fabricated on NCPSS and on the planar substrate, measured at 15 K. Regardless of the variation of the sapphire substrate, a very strong emission peak at 2.8–2.9 eV (442–427 nm) was observed for both specimens. However, a smaller full width at half-maximum (FWHM) of PL spectra of approx-

 © 2010 The Japan Society of Applied Physics

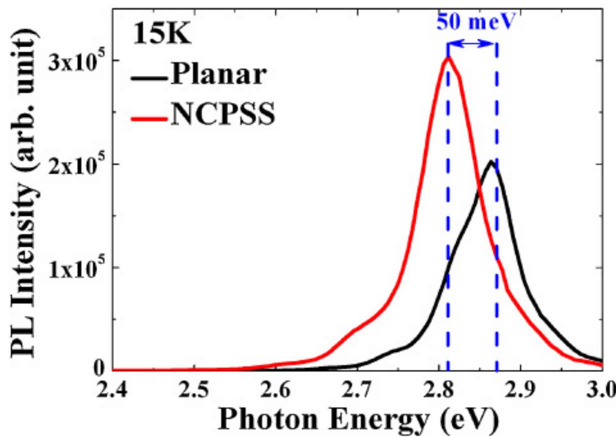

Fig. 5. (Color online) 15 K PL spectra of GaN-based LEDs fabricated on NCPSS and planar substrate.

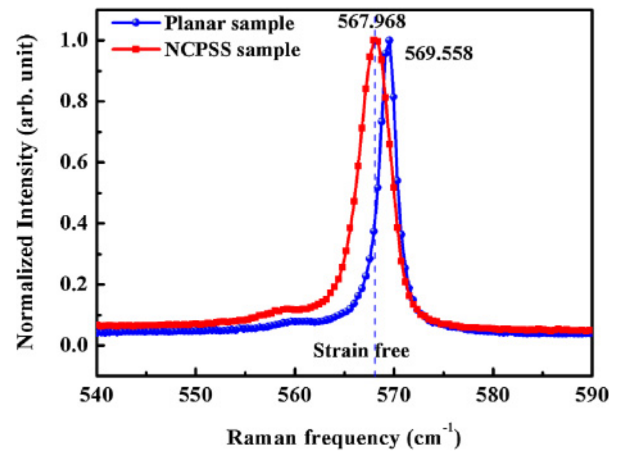

Fig. 6. (Color online) Room-temperature Raman spectra for GaN-based LED fabricated on NCPSS and planar substrate.

imately 89 meV at 15 K was obtained from the GaN-based LED fabricated on NCPSS. Otherwise, the PL intensity of the GaN-based LED fabricated on NCPSS is stronger than that of the GaN-based LED fabricated on the planar sapphire substrate by a factor of 2, and the emission peak energy exhibited an appreciable redshift of about 50 meV. As is common knowledge, the strain in the epilayer, arising from the large lattice mismatch, will induce the quantum-confined-Stark effect (QCSE). In other words, the strain can reduce the radiative recombination rates of electrons and holes, and consequently, the PL luminescence intensity of the specimen will be decreased. Moreover, we used the high-resolution XRD experimental and fitted scans of InGaN/GaN MQWs grown on the planar substrate and NCPSS. There is a difference in the indium composition between the two MQW samples. For the InGaN/GaN MQWs grown on NCPSS, the In composition is 10%, which is greater than that on the planar substrate (8%). Moreover, the Raman shift indicated that the strain of the NCPSS sample is less than that of the planar sample, as shown in Fig. 6. According to the report of Zang *et al.*, the In content of InGaN wells in the GaN-based LED is associated with the degree of strain in the epilayer.[18] Therefore, on the basis of the above-mentioned results, we hypothesize that the redshift behavior and stronger PL luminescence may be associated with the higher In content and weaker QCSE, respectively, resulting from the reduction of the strain in the epilayer.

Figures 7(a) and 7(b) show the room-temperature excitation power dependence of emission energy and FWHM of GaN-based LEDs fabricated on NCPSS and the planar substrate. As we can see, for all samples, the trend of data can be separated into three regions, denoted as regions I, II, and III. These three regions are divided by red dash lines, as shown in Fig. 7. For region I, the emission energy and FWHM of the PL spectrum decrease with increasing excitation power. In general, the recombination of carriers includes two process at room temperature: one can be attributed to radiative recombination; the other can be attributed to nonradiative recombination, i.e., compensation of nonradiative centers. In other words, most of the excited carriers will be confined and will recombine at nonradiative centers. In addition, the excited carriers will fill the nonradiative centers. Thus, the emission energy shows

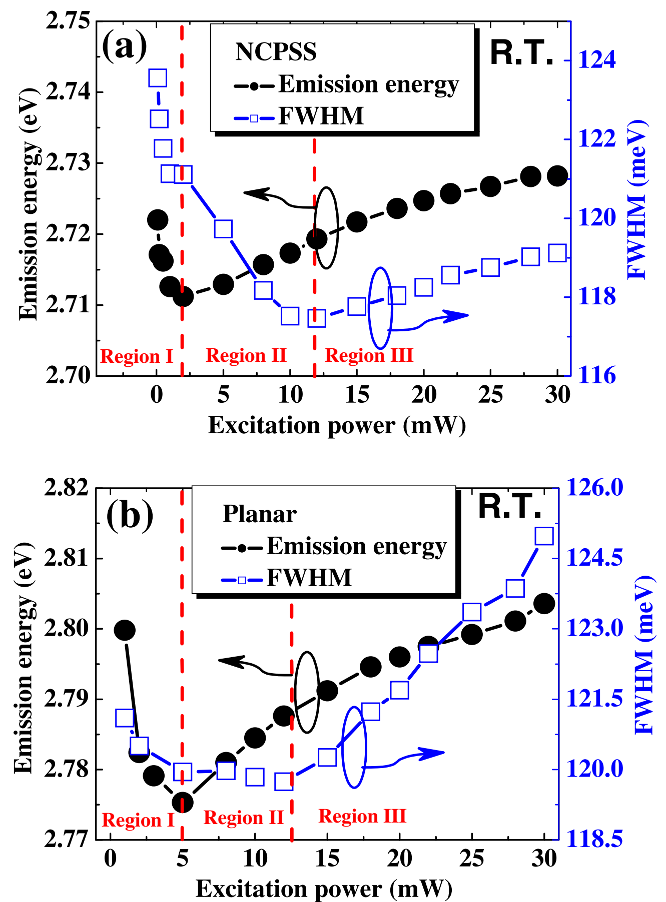

Fig. 7. (Color online) Variation of emission energy and full width at half-maximum with excitation power at 300 K for GaN-based LEDs fabricated on (a) NCPSS and (b) planar substrate.

redshift and FWHM decreases with increasing excitation power first. According to the results of a past study, this behavior is mainly attributed to the compensation of nonradiative centers.[19,20] When the excitation power kept increasing, the nonradiative recombination centers were gradually bleached out. Hence, the trend in Fig. 7 was changed from region I to region II and the radiative recombination became the dominant process. For region II, the FWHM of the PL spectrum decreases with increasing

© 2010 The Japan Society of Applied Physics

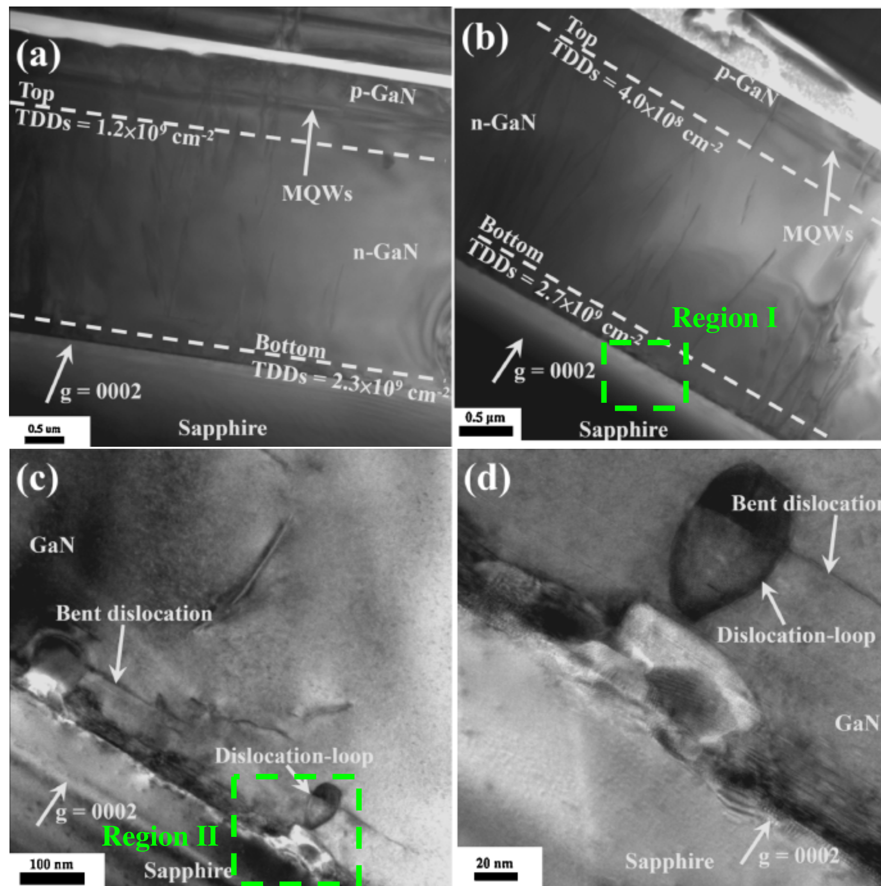

Fig. 8. (Color online) TEM cross-sectional images of epitaxial structure of GaN-based LED with the projection along [01$\bar{1}$1]: (a) fabricated on planar substrate; (b) fabricated on NCPSS; (c) HRTEM image of region I in (b); and (d) a magnified view of region II in (c). The diffraction condition is $g = 0002$.

excitation power, while the emission energy of the PL spectrum increases. This is because the strain-induced piezoelectric field in MQWs can be screened by photo-generated carriers, resulting in the weakening of the QCSE. Therefore, the emission energy shows blue shift and FWHM decreases with increasing excitation power. Finally, for region III, the emission energy and FWHM of the PL spectrum increase with increasing excitation power. At higher excitation power, the strain-induced piezoelectric field seems to be fully screened and FWHM no longer decreases. Consequently, band filling is dominant, which can also lead to emission energy blue shift and the broadening of the FWHM. Thus, this can well explain the change in the FWHM and the energy of the PL peak.

From the same figure, it can also be found that the excitation power of the turning point between region I and region II for the NCPSS specimen is lower than that for the planar specimen, indicating that the threading dislocation density of the GaN-based LED fabricated on NCPSS is lower than that of the GaN-based LED fabricated on the planar substrate. Furthermore, for region III in Fig. 7, the FWHM of the PL spectrum increases to approximately 1.7 and 5.3 meV for NCPSS and planar samples, respectively, and the emission energy of specimens shifts toward higher emission energy, resulting in approximately 8.9 and 16 meV blue shift for the GaN-based LED fabricated on NCPSS and the planar substrate, respectively. Again, the NCPSS sample has lower TDDs owing to its having the smallest broadening degree and weaker carrier localization degree.

Figure 8 presents cross-sectional TEM images of the GaN-based LED fabricated on NCPSS and the planar substrate. A comparison of Figs. 8(a) and 8(b) shows that the dislocation density is more effectively reduced in the NCPSS sample than in the planar sample. In other words, the n-GaN epilayer grown on the planar substrate has many dislocations threading through the multiple quantum wells (MQWs) to the top surface of the epilayer. The TDD for this specimen is estimated to be 2.3×10^{9} cm^{-2} at the bottom of the n-GaN layer, and it decreases to 1.2×10^{9} cm^{-2} at the top of the n-GaN layer and 6.2×10^{8} cm^{-2} in the p-GaN region. Otherwise, for the epilayer grown on NCPSS, far fewer dislocations are observable within the range of view. As shown in Fig. 8(b), the TDD at the bottom of the n-GaN layer is about 2.7×10^{9} cm^{-2}; however, the TDD at the top of the n-GaN layer decreases to 4.0×10^{8} cm^{-2}, and it is only 8.8×10^{7} cm^{-2} in the p-GaN region. To confirm the crystallinity of the GaN-based LED fabricated on NCPSS and observe more clearly the dislocation behavior in the epilayer, the enlargements of region I in Fig. 8(b) and region II in Fig. 8(c) are presented in Figs. 8(c) and 8(d), respectively. As can be seen in Fig. 8(c), many bent dislocations accompany the dislocation loops in the interface between GaN and sapphire. However, their extension into the epilayer was mostly suppressed. A possible mechanism of the defect reduction is considered to include the following: the GaN epilayer grown on an uneven substrate can cause the crystal lattice to experience repeated compressive and tensile stress, initializing the migration and bending of

 © 2010 The Japan Society of Applied Physics

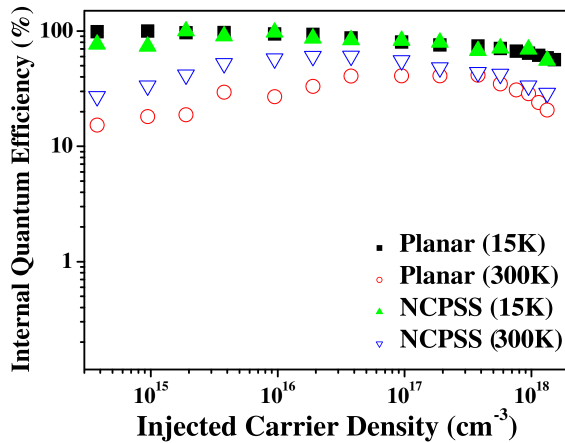

Fig. 9. (Color online) Internal quantum efficiency as a function of injected carrier density for GaN-based LEDs fabricated on NCPSS and planar substrate measured at 15 and 300 K.

the misfit dislocations. Hence, the probability of dislocation–dislocation interactions is increased, and dislocation loops form, as shown in Fig. 8(d), reducing the number of misfit dislocations that thread into the n-GaN, MQWs, and p-GaN epilayers.[21–26)]

Finally, the IQE of GaN-based LEDs fabricated on NCPSS and the planar substrate was determined, as shown in Fig. 9, measured as the ratio of the integrated PL intensity from the active layer of the specimen at 300 K to the integrated PL intensity at 15 K.[27)] As demonstrated, the IQE of the GaN-based LED fabricated on NCPSS is as high as 48% at 30 mW (injected carrier density $= 2 \times 10^{17}$ cm^{-3}),[20)] corresponding to a current of 20 mA, which is higher than that of the GaN-based LED fabricated on the planar substrate by 8%. Therefore, the use of NCPSS is suggested to be effective for elevating the emission efficiency of GaN-based LEDs owing to the improvement in crystal quality.

4. Conclusions

A high-performance GaN-based LED was fabricated on NCPSS by LP-MOCVD. The RMS value of surface roughness of the GaN-based LED fabricated on NCPSS was approximately 1.18 nm, as determined by atomic force microscopy. From the 15 K PL measurement, the PL intensity of the GaN-based LED fabricated on NCPSS was found to be stronger than that of GaN-based LED fabricated on the planar substrate by a factor of 2. In addition, the emission peak energy exhibited appreciable redshift of about 50 meV. According to the results of past studies, the specimen showing redshift behavior and stronger luminescence is probably associated with less strain, suggesting that GaN-based LED of good quality was fabricated on NCPSS. Moreover, TEM characterizations exhibited far fewer dislocations within the overall range of view for the GaN-based LED fabricated on NCPSS. The threading dislocation density in the bottom n-GaN layer was about 2.7×10^9 cm^{-2}; however, it decreased to 4.0×10^8 cm^{-2} in the top n-GaN layer and was only 8.8×10^7 cm^{-2} in the top p-GaN region. Hence, we confirmed that the result of lower TDD on NCPSS is due to the formation of dislocation loops. Finally, a GaN-based LED was produced on NCPSS. It demonstrated an internal quantum efficiency of 48%, which is superior to those produced on planar substrates by about 8%. Therefore, NCPSS can offer advantages to GaN-based LEDs, such as reduced dislocation density and enhanced emission efficiency.

Acknowledgment

The authors are grateful to the National Science Council of the Republic of China, Taiwan, for financially supporting this research under Contract No. NSC 96-2221-E009-067.

1) Y. Narukawa, I. Niki, K. Izuno, M. Yamada, Y. Murazki, and T. Mukai: Jpn. J. Appl. Phys. **41** (2002) L371.
2) E. F. Schubert: *Light Emitting Diodes* (Cambridge University Press, Cambridge, U.K., 2003) 2nd ed., p. 21.
3) J. Han, M. H. Crawford, R. J. Shul, J. J. Figiel, L. Zhang, Y. K. Song, H. Zhou, and A. V. Nurmikko: Appl. Phys. Lett. **73** (1998) 1688.
4) S. Nakamura, M. Senoh, S. Nagahama, N. Iwasa, T. Yamada, T. Matsushita, H. Kiyoku, Y. Sugimoto, T. Kozaki, H. Umemoto, M. Sano, and K. Chocho: Appl. Phys. Lett. **72** (1998) 211.
5) D. Kapolnek, S. Keller, R. Vetury, R. D. Underwood, P. Kozodoy, S. P. Den Baars, and U. K. Mishra: Appl. Phys. Lett. **71** (1997) 1204.
6) T. S. Zheleva, O.-H. Nam, M. D. Bremser, and R. F. Davis: Appl. Phys. Lett. **71** (1997) 2472.
7) D. M. Follstaedt, P. P. Provencio, N. A. Missert, C. C. Mitchell, D. D. Koleske, A. A. Allerma, and C. I. H. Ashby: Appl. Phys. Lett. **81** (2002) 2758.
8) A. Sakai, H. Sunakawa, and A. Usui: Appl. Phys. Lett. **71** (1997) 2259.
9) T. S. Zheleva, O. H. Nam, M. D. Bremser, and R. F. Davis: Appl. Phys. Lett. **71** (1997) 2472.
10) D. S. Wuu, W. K. Wang, K. S. Wen, S. C. Huang, S. H. Lin, S. Y. Huang, C. F. Lin, and R. H. Horng: Appl. Phys. Lett. **89** (2006) 161105.
11) Y. J. Lee, J. M. Hwang, T. C. Hsu, M. H. Hsieh, M. J. Jou, B. J. Lee, T. C. Lu, H. C. Kuo, and S. C. Wang: IEEE Photonics Technol. Lett. **18** (2006) 1152.
12) Z. H. Feng, Y. D. Qi, Z. D. Lu, and K. M. Lau: J. Cryst. Growth **272** (2004) 327.
13) T. V. Cuong, H. S. Cheong, H. G. Kim, H. Y. Kim, C.-H. Hong, E. K. Suh, H. K. Cho, and B. H. Kong: Appl. Phys. Lett. **90** (2007) 131107.
14) H. Gao, F. Yan, Y. Zhang, J. Li, Y. Zeng, and G. Wang: J. Appl. Phys. **103** (2008) 014314.
15) A. Xing, M. Davanco, D. J. Blumenthal, and E. L. Hu: J. Vac. Sci. Technol. B **22** (2004) 70.
16) D. S. Wuu, W. K. Wang, K. S. Wen, S. C. Huang, S. H. Lin, R. H. Horng, Y. S. Yu, and M. H. Pan: J. Electrochem. Soc. **153** (2006) G765.
17) H. W. Huang, C. H. Lin, C. C. Yu, B. D. Lee, C. H. Chiu, C. F. Lai, H. C. Kuo, K. M. Leung, T. C. Lu, and S. C. Wang: Nanotechnology **19** (2008) 185301.
18) K. Y. Zang, Y. D. Wang, H. F. Liu, and S. J. Chua: Appl. Phys. Lett. **89** (2006) 171921.
19) Y. H. Cho, G. H. Gainer, A. J. Fischer, J. J. Song, S. Keller, U. K. Mishra, and S. P. DenBaars: Appl. Phys. Lett. **73** (1998) 1370.
20) Y. J. Lee, C. H. Chiu, C. C. Ke, P. C. Lin, T. C. Lu, H. C. Kuo, and S.-C. Wang: IEEE J. Sel. Top. Quantum Electron. **15** (2009) 1137.
21) I. Ma'rtil, E. Redondo, and A. Ojeda: J. Appl. Phys. **81** (1997) 2442.
22) X. A. Cao, E. B. Stokes, P. M. Sandvik, S. F. LeBoeuf, J. Kretchmer, and D. Walker: IEEE Electron Device Lett. **23** (2002) 535.
23) X. Q. Shen, M. Shimizu, and H. Okumura: Jpn. J. Appl. Phys. **42** (2003) L1293.
24) X. Q. Shen, K. Furuta, N. Nakamura, H. Matsuhata, M. Shimizu, and H. Okumura: J. Cryst. Growth **301–302** (2007) 404.
25) X. Q. Shen, H. Okumura, K. Furuta, and N. Nakamura: Appl. Phys. Lett. **89** (2006) 171906.
26) X. Q. Shen, H. Matsuhata, and H. Okumura: Appl. Phys. Lett. **86** (2005) 021912.
27) S. Watanabe, N. Yamada, M. Nagashima, Y. Ueki, C. Sasaki, Y. Yamada, T. Taguchi, K. Tadatomo, H. Okagawa, and H. Kudo: Appl. Phys. Lett. **83** (2003) 4906.

© 2010 The Japan Society of Applied Physics